Desalination 608 (2025) 118784

Contents lists available at ScienceDirect

Desalination

journal homepage: www.elsevier.com/locate/desal

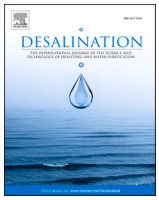

Renewable energy powered membrane technology: Electro-hydraulic control system design for managing pump shutdowns in a photovoltaic-membrane water desalination system

Emmanuel O. Ogunniyi, Bryce S. Richards *

Institute of Microstructure Technology (IMT), Karlsruhe Institute of Technology, Hermann-von-Helmholtz-Platz 1, 76344 Eggenstein-Leopoldshafen, Germany

HIGHLIGHTS

- A PV power relative deviation ≥30 %/s causes electrical shutdowns of the pump
- Electro-hydraulic control system (EHCS) facilitates valve response & shutdown control
- PV-membrane: EHCS increased daily production, 7.5 % BW30 & 14.6 % NF90 on cloudy day
- EHCS reduced more shutdowns with low-permeability BW30 (86 %) vs. NF90 (57 %)
- Direct pressure accumulator buffering, ineffective for r/trip efficiency & pump shutdowns

GRAPHICAL ABSTRACT

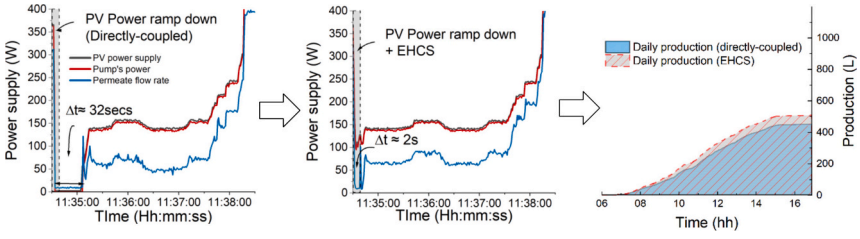

ARTICLE INFO

Keywords:
Actuator valve
Electrohydraulic control
Energy buffering
Pressure accumulator
Ramp-rate
Reverse osmosis
Shutdown

ABSTRACT

The electrical shutdown of the pump during the period of solar irradiance (SI) fluctuations is one of the major challenges of a photovoltaic-powered membrane desalination (PV-membrane) system, leading to intermittent operation, reduced daily production and lower water quality. Conventional energy buffering methods, using electrical storage (batteries or supercapacitors) or mechanical storage (pressure accumulators), provide only temporary buffering, however, cannot prevent pump shutdowns. Direct control of PV-membrane hydrodynamics, independent of energy buffering systems, remains an underexplored solution to this issue. In this study, an electrohydraulic control system (EHCS) was developed to dynamically minimise pump shutdowns during unfavorable weather conditions across different membrane types. The system achieves this by rapidly reducing the load pressure on the pump via fast-response control actions using an electrically actuated valve. Experimental results demonstrate that the EHCS (without buffering support) increased daily water production by 7.5 % for the BW30 membrane and 14.6 % for the NF90 membrane under highly cloudy conditions. Additionally, pump shutdowns were reduced by 86 % for the BW30 membrane and 57 % for the NF90 membrane. The findings highlight the EHCS as an effective alternative for managing PV-membrane system performance during SI fluctuations, offering a robust solution without reliance on energy buffering systems.

* Corresponding author.
E-mail address: bryce.richards@kit.edu (B.S. Richards).

https://doi.org/10.1016/j.desal.2025.118784
Received 7 January 2025; Received in revised form 25 February 2025; Accepted 5 March 2025
Available online 6 March 2025

1. Introduction

1.1. Potential of small-scale renewable-energy-powered membrane desalination systems

With the current world population growth rates (about 71 million people per year [1], projected at 10 billion people by 2050 [2,3]) and the resulting decline in freshwater availability-to-groundwater ratio (currently about 40 % [4]), the global water demand is projected to increase by 20–25 % globally by the year 2050 [5]. This trend is currently leading to increased global water scarcity, where access to sufficient water for personal and domestic use – which is safe, acceptable, and affordable – is <50 l per person per day in most places in the world, especially in the arid and semi-arid regions [5–7]. This has driven the exploration of alternative portable methods for clean water production through desalination [8], such as small-scale renewable-energy-powered membrane desalination systems. Small-scale (e.g. daily production capacity of about 3000 L [9]) renewable-energy-powered membrane desalination systems can offer a promising decentralised water solution to address water scarcity in off-grid or remote areas which typically lack access to an electricity grid. This naturally will also assist in meeting the United Nations Sustainable Development Goals 6 & 7 of promoting clean energy and access to clean drinkable water [10,11].

Although there are various renewable energy sources, such as solar photovoltaic (PV), wind, and hydro [12], PV energy is mostly preferred for membrane-based systems due to its reliability, scalability, and low maintenance [9]. However, PV-powered membrane desalination (PV-membrane) systems face challenges from solar irradiance (SI) fluctuations, which disrupt power supply, affecting the system's daily performance and production capacity [13–15].

1.2. Photovoltaic power fluctuations and pump shutdowns

PV power ramp-down caused by SI fluctuations, can significantly affect both the electrical and hydraulic performance of PV-membrane systems. In a directly-coupled PV-membrane system (i.e. with no energy storage components), when the available PV power supply falls below the minimum demand by the pump, P_{pump_min}, to generated sufficient pressure to overcome the transmembrane pressure TMP (net driving pressure plus the osmotic pressure of the salt water [16]), the pump shuts down. This is followed by a period of dead-time before restarting, during which no permeate (drinkable water) production occurs, thus impairing the daily production. Additionally, a pump shutdown may occur when the magnitude of PV power ramp-down, relative to the initial power supply, ΔP_{PVrel} exceeds the maximum power ramp-rate that can be tolerated by the pump in one second, rr_{pump_max} /s), as defined in Eq. (1):

$$\Delta P_{PVrel}\ (\%/s) = \left| \frac{P(t) - P(t-\Delta t)}{P(t-\Delta t)} x100\% \right| > rr_{pump\_max}\ (W/s) \quad (1)$$

This shutdown can occur even if the new power level after ramp-down event P(t) remains above the pump's minimum power demand. Protective electronics in most electrical pumps trigger this the shutdown to prevent motor damage, and the specific maximum allowable ramp-rate threshold of the pump $rr_{pump_{max}}$ can be determined through empirical ramp-rate testing of the chosen pump. Since PV power ramp-rate cannot be directly influenced, as it depends on SI fluctuations, in most power control systems, the ramp-rate per second *(ΔP/s)* or the relative PV power ramp-rate ΔP_{PVrel} is often used to implement control conditions for improving power stability in PV-powered systems [17–20]. In PV-membrane systems where controlling the shutdown of the pump is important, the implementation of relative ramp rates is crucial for controlling the pump as the rr_{pump_max} can be consistent across various levels of PV power fluctuations, thus enabling flexibility of pump control.

Desalination membranes – such as reverse osmosis (RO) and nanofiltration (NF) – meanwhile can perform better when operated continuously under steady-state conditions, especially with no continuous pump shutdowns [21,22]. When powered by renewable energy such as solar or wind, which are subject to fluctuations and intermittencies [23–27], it is important to maintain the pressure stability and prevent pump shutdowns towards ensuring consistent and enhanced system performance [28]. One common approach of realising this (maintaining pressure stability and preventing the pump's shutdowns) is by integration of energy buffering using electrical energy storage (EES) (e.g., batteries or supercapacitors), or mechanical energy storage (MES), such as pressure accumulators [18,29–34]. Another approach involves oversizing renewable energy sources or anti-correlating the hybrid renewable sources (especially wind and solar) to ensure more power is produced during unfavorable weather conditions [35,36]. The disadvantages here however include: i) a significant increase in system design cost; and ii) the system not very feasible in space-constrained environments; and iii) possibility of excess electricity produced being unutilised by the system during peak power generation.

1.3. Electrical and mechanical energy buffering in PV-membrane systems

1.3.1. Electrical energy storage (EES) buffering and sizing for PV-membrane

The use of EES – such as battery, supercapacitor (SC) or hybrid of both – have been demonstrated to enable power buffering and enhance the performance of PV-membrane water desalination system during low or fluctuating SI conditions [18,32,34,37,38]. However, a few challenges associated with this can limit their full potential for PV-membrane system. These include degradation, limited storage capacity and energy loss during power storage and conversion as detailed below [39–46]:

The storage capacity battery degrades over time, depending on the pattern of usage [41], thus necessitating periodic replacements, for example Li-ion battery shelf life is about ≥6 years [47]. The SC on the other hand is limited with low energy density of about 0.1 to 60 Wh/kg. This is low when compared to battery storage, e.g. 90–260 Wh/kg for Li-ion battery [43–45]. Due to this low energy density, commercially available high energy density SC, which can be comparable to battery attracts high cost, and this can increase the overall system design cost when SC only or battery/SC hybrid is used for energy buffering.

Additionally, Electrical energy loss can occur due to the limited round-trip efficiency of the EES, (for example, this is typically 82–95 % for commercial Li-ion battery [40,42]), as well as the conversion loss through the charge controller during EES charging [39]. During operation, conversion of the stored energy in EES into hydraulic energy goes through mechanical losses due to the pump's limited efficiency (e.g. 42–76 % efficiency for helical rotor pump which is mostly used in PV-powered water pumping systems [9,48–51]). These can reduce the daily energy utilisation during buffering operation.

Meanwhile, the sizing of EES buffering power (P_{ESS}) for PV-membrane applications is based on the system design configurations using the maximum load demand (here represented as pump power demand, P_{Pump}, at maximum head as the main electrical load in the system), and the available maximum power from the PV panels (P_{PV}). The ESS sizing and iteration process for buffering can thus be formulated using mathematical relations as adapted from Caro-Ruiz et *al.* [52], and be calculated based on the total estimated PV power required over a certain time duration, as resented in Eqs. (2) and (3).

$$P_{ESS} = max\left|P_{Pump}(t) - P_{PV}(t)\right| \quad (2)$$

$$C_{ESS} = \int_{t}^{t+1} (P_{ESS})dt \quad (3)$$

1.3.2. Mechanical energy storage (MES) buffering sizing for PV-membrane

MES refers to systems that store potential or kinetic energy in a mechanical form. One common type of MES is a pressure accumulator, which is ideal for short-term storage (seconds to a few minutes) and can find application in renewable energy powered system during intermittent power supply. Other MES types can store energy on a larger scale for longer durations or grid applications, and these include compressed air energy storage, flywheel energy storage, pumped hydroelectric storage [31]. A pressure accumulator (also known as "bladder tank") can provide direct pressure buffering to improve the performance of pressure-driven systems where fluctuating power supply causes pressure variations in the system [53–58].

Although pressure accumulators seem to be less explored in PV-membrane systems, these have been utilised in some studies for feed water pressure buffering and ultrafiltration backwash applications across various configurations [33,53,59–61]. For instance, Mi et al. [60] used a pressure accumulator to address feed pressure fluctuations in a wind-powered seawater RO desalination system, but motor pressure was insufficient at low wind speeds (<4.5 m/s), exacerbating pressure gradients during buffering. Karavas et al. [53] employed a three-parallel pressure vessel array (180 L capacity) for short-term energy buffering, producing 17 L of permeate in 20 min, though continuous PV recharging and daily performance were not studied. Villessot et al. [33] patented a battery-less system using a pressure accumulator to buffer PV power drops, integrating hybrid power sources for continuous operation which limits PV-only autonomy. Li et al. [61] demonstrated a pressure accumulator's effectiveness in ultrafiltration backwash under varying solar irradiance conditions.

The sizing of MES for buffering in PV-membrane systems is mostly determined by the system's pressure (p) and flow rate (Q) requirements. The buffering duration depends on the accumulator's size (volume). Large hydraulic accumulators, however, face challenges such as significant space requirements, slow pressure buildup during charging, and potential hazardous failures due to pressurised fluid. For short-term hydraulic buffering (e.g., up to 5 min) during pump shutdowns, the charged volume at any time t in the accumulator V(t) can be described by the polytropic process Eq. (4).

$$p_i V_i^n = p_t V_t^n \tag{4}$$

where p_iV_i are the initial pressure and volume, p_tV_t are the pressure and volume at time t, n is the polytropic index (e.g $n = 1.4$ for adiabatic processes with no heat exchange). The sizing of pressure accumulator in PV-membrane system in this study is determined based on the charged volume, which is a function of the feed flow rate supplied by the pump, and the buffering time. These are described in Eqs. (5) and (6).

$$\left.\begin{aligned} V_t &= V_i + \int_0^t Q_f(t)dt \\ &\quad or \\ V_t &= V_i + (\mathrm{A} \bullet v \bullet t) \end{aligned}\right\} \tag{5}$$

where A is the pipe's cross-sectional area, v is the flow velocity, and the buffering time t can then be estimated as:

$$t = \frac{V(t) - V_i}{\mathrm{A} \bullet v} \tag{6}$$

While pressure accumulators are generally applied for pressure buffering, most studies have not investigated their impact on pump electrical shutdowns in PV-membrane systems. Furthermore, system shutdowns may still occur during the accumulators' charging or discharging phase, especially under low PV power conditions when pump's feed pressure is insufficient to overcome the membrane's osmotic pressure.

1.4. Direct hydraulic pressure regulation in an unbuffered PV-membrane system

Considering the limitations of both EES and MES in providing a sustaining and efficient buffering support for PV-membrane systems, an alternative hydraulic control strategy can be explored to prevent pump shutdowns without relying on additional energy storage. One potential approach involves strategically controlling the hydrodynamics of the PV-membrane system, specifically by regulating flow rate and pressure. By continuously varying the total hydraulic load or adjusting the operating setpoint (pump head), the total hydraulic height (or pressure) the pump must overcome during periods of low PV power supply can be reduced, thus minimising the risk of pump shutdowns. This can be achieved by dynamically adjusting the backpressure valve of the PV-membrane system. When an electrically controlled actuator valve is used for this purpose, it can be programmed to adjust continuously in response to PV power ramp rates.

The use of controlled actuator valves offers a novel solution to prevent shutdowns in PV-membrane systems. Traditionally, pump speed control relies on variable frequency drives (VFDs) that adjust AC motor frequency [62,63]. However, VFDs are inefficient for DC-powered pumps due to the possibility of energy losses during DC-to-AC conversion. Meanwhile, Mendonça et al. [64] proposed a self-regulating diaphragm valve and charge controller for pressure regulation, but this cannot prevent shutdowns during PV power fluctuations. Similarly, Ma et al. [65] implemented open/close valve control with multiple pumps to reduce fouling in nanofiltration, but the on/off operation limits precise flow and pressure regulation.

1.5. Research questions

This study thus proposes an electro-hydraulic control system (EHCS) that employs an electrical actuator valve (AV) which is controlled to directly regulate the hydrodynamics (flow and pressure) of a PV-membrane system, dynamically preventing pump shutdowns during PV power ramp-down events. In addition, mechanical energy buffering using a pressure accumulator is investigated to assess the effectiveness of direct pressure buffering in PV-membrane system. The potential challenges that could arise with this approach and a possible hybrid combination with the EHCS are further explored across different SI conditions for PV-membrane system.

To realize these, the following research questions are investigated:

i. How can the hydraulic parameters of a PV-membrane system be directly regulated (e.g. with an actuator valve) to minimise or prevent the electrical shutdowns of the pump during PV power ramp-down events on different solar days?
ii. Can direct pressure buffering using a pressure accumulator be integrated with a valve control method to enhance PV-membrane system performance while preventing both electrical and hydraulic shutdowns?
iii. What are the possible specific limitations of the direct hydraulic buffering and control approaches (with pressure accumulator and/or actuator valve), when implemented for different membrane types under different SI conditions in PV-membrane system?

2. Materials and methods

The PV-membrane system in this work was modified via the addition of a pressure accumulator and an electrical actuator valve – two different strategies to mitigate or minimise system shutdowns. The study also investigated the effect of these components on flow pressure regulation without relying on energy storage methods. The operational logic of the system was managed by a programmable logic controller (PLC) which enables real-time optimisation of system parameters with respect

to specific operational conditions. The system configurations, descriptions, and methods are provided in this section.

2.1. PV-membrane system setup and descriptions

The system configurations utilised in this study are depicted in Fig. 1. The materials used are categorised and described under two main components: Electrical and hydraulic. The electrical components include PV panels, pump, valves, sensors, and PLC, while the hydraulic components encompass the membrane filtration unit and pressure accumulator. The main system components of the designed PV-membrane system are summarised in Table I.

These days were selected for consistency with previous studies [66] and represent different irradiance conditions in KIT Germany: i) a "sunny day" (5 May 2016) with no cloud cover, ii) a "partly cloudy day" (26 May 2016) characterised by intermittent heavy clouds during midday, and iii) a "very cloudy day" (13 October 2016), representing a near worst-case scenario in this study.

In addition to the summarised components, the following sensors are used in the system: Pressure (Bürkert 831), electrical conductivity EC (Bürkert 8222), Flow sensor (Bürkert8030; Kobold MIM-12); current sensor (Phoenix Contact MCR-S10–50); voltage sensor (Omega DRST-CM 300), and solid-state relays SSRs (TC-GSR1-40DD). The interconnections of these components and a detailed system description are provided in the Supplementary Information **S1**.

The PV-membrane system was designed to investigate the optimal method of controlling pump shutdowns during SI fluctuations on cloudy days. This was studied using two different membrane types with varying permeabilities, BW30 and NF90, while the system control was managed via a PLC.

2.2. Experimental and control methods

The key electrical components controlled in this study are the actuator valve and the bypass normally-closed (NC) solenoid valve. The actuator valve receives analogue signals from the PLC to regulate its degree of opening, while the NC solenoid valve operates using digital signals from the PLC to toggle between its on and off states. The primary hydraulic component is the pressure accumulator, which serves as a pressure buffer. The charging and discharging of the accumulator are managed through NC valves located at the inlet and outlet channels. These valves are controlled by digital signals from the PLC, based on the set operating conditions. The control methods for these electrical and hydraulic components are described in this section.

2.2.1. Electrical actuator valve control method

In membrane systems, a valve is installed on the concentrate stream primarily to regulate the back pressure and concentrate flow rate. When the back-pressure valve restricts the concentrate flow, the increased hydraulic resistance requires the pump to consume more power and raise the feed pressure to overcome it. The higher feed pressure increases the recovery rate (the ratio of permeate to feed flow). Conversely, when the valve is relaxed, more flow is diverted through the concentrate channel, reducing the pressure needed for permeate production (and recovery) and thereby lowering the pump's power demand.

An electrical actuator valve (AV), installed on the concentrate stream (Fig. 1), is used for back pressure control valve in this study, as this allows precise hydraulic flow control and automated operation. While the AV offers precise pressure control, its motorised mechanism could cause a slow response time (>1 s) in adjusting stroke length to the desired setpoint. To address the need for rapid pressure adjustments critical for shutdown control, a normally-closed solenoid valve (NC3, Fig. 1) is installed as a bypass across the AV. A levered ball valve (BV), positioned before the solenoid valve NC3 regulates the allowable pressure diversion through the bypass.

The control of the AV and BV is implemented using an on/off control strategy within a closed-loop feedback control system, as illustrated in Fig. 2. This strategy evaluates the error between real-time PV power fluctuations and the predefined maximum relative PV power deviation. The signal is processed by the PLC, which outputs a digital on/off signal to regulate the bypass valve. Meanwhile, the actuator valve receives an analogue signal to adjust its position according to a new setpoint.

Since not all PV power ramp-downs result in pump shutdowns, the maximum ramp-down threshold that could trigger a pump shutdown (P_{PVsd}) is experimentally determined. This threshold is used together with the PV power supply level (P_{PV}), as logic inputs to regulate the actuator valve's opening and closing. The control algorithm for this process is depicted in Fig. 3.

As shown in Fig. 3, the algorithm monitors the PV power ramp-rate ($\Delta P_{PV}/\Delta t$) to determine when the PV power supply (P_{PV}) reaches a

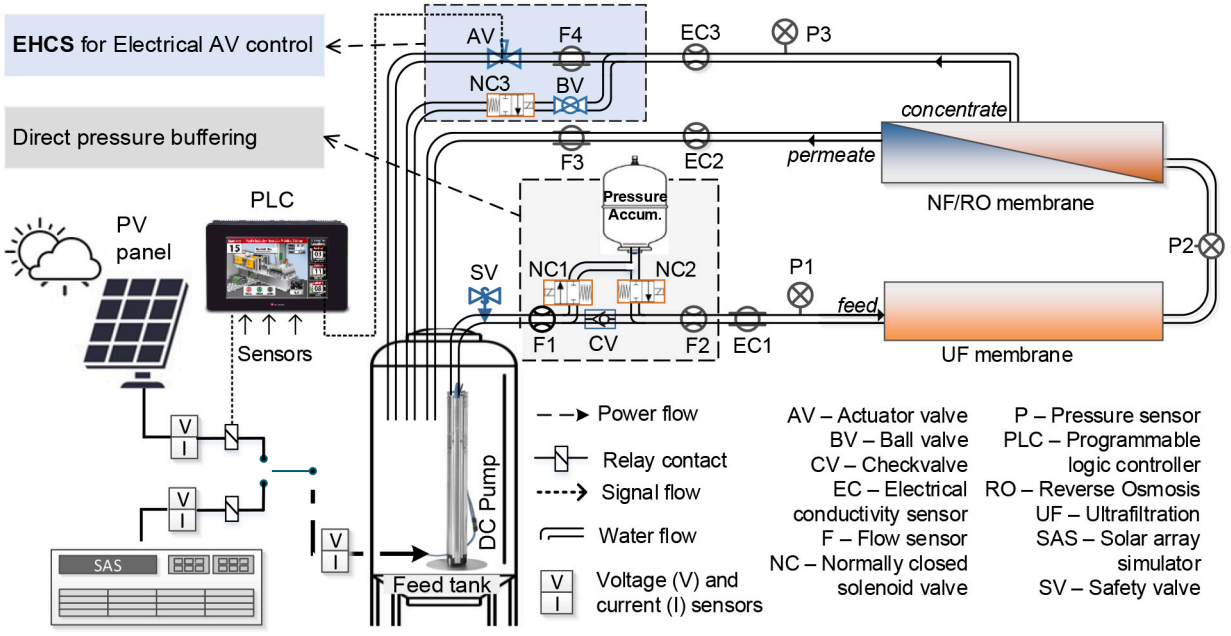

Fig. 1. PV-membrane system setup with integrated actuator valve and pressure accumulator for shutdown control during SI fluctuations.

Table I
Summarised PV-membrane system components.

Component	Electrical components						Hydraulic components		
	PV panel	Solar array simulator (SAS)	Solar days	Electric pump	Actuator valve	PLC	Pressure accumulator	Brackish feed water	Membranes
Type	Offgridtec flexible silicon	Chroma 62050H 600S	1) sunny, 2) partly cloudy, 3) very cloudy	Grundfos SQFlex 0.6–2 N helical rotary	Hanbay MCL S50-AB 24 V SS	Unitronics Unistream 10.4"	Reflex Refix DD 25	Deionised water +5 g/L NaCl	Inge: UF; DuPont FilmTec: NF90, BW30
Rating/ source	100 W P_{mp}; 39.6 V V_{mp}	5 kW max	KIT solar park data (2016)	12 bar, 590 L/h, 420 W max	24 V DC	24 V DC power, 4–20 mA inputs	18.7 L, 4 bar pre-charge pressure	270 L; 2.09 bar osmotic pressure at 20 °C	UF: 6.0 m^2, TMP 0.1 - 2 bar; NF90 & BW30: 7.2m^2, 41 bar.
Configuration	3 series / 2 parallel (600 W_p; 118.8 V_{mp})	Program: with real solar days	Varying levels of SI fluctuations	Directly coupled to PV array	PV-membrane back-pressure control	Analogue inputs; analogue & digital outputs	Between pump & UF membrane	Permeate & concentrate recycled back into feed	UF + NF90 or UF + BW30

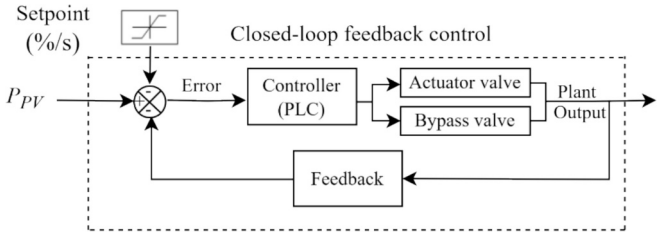

Fig. 2. Closed-loop on/off control strategy for valve control.

certain minimum threshold (P_{PVmin}), which is sufficient for the membrane to produce drinkable permeate. If the ramp-rate exceeds the shutdown threshold (P_{PVsd}), the AV adjusts to a lower setpoint, and the bypass solenoid valve triggers momentarily to prevent system shutdown. Once the ramp-down condition is resolved, the valve returns to its initial setpoint, ensuring system stability and continuous operation.

2.2.2. Pressure accumulator control method

The pressure accumulator implemented in this work (already introduced in Section 2.1.2a) is installed between the feed pump and the UF membrane as shown in Fig. 1, to buffer the feed pressure fluctuations due to low or fluctuating PV power supply to the pump during SI fluctuations.

The buffering is done by controlling the discharge of the tank when the feed pressure drops below a certain pressure threshold. When the pump generates a feed pressure (p_f) lower than the set minimum threshold (P_{fmin}) during the PV power ramp-down events, the pressure accumulator is enabled for discharging as long as the pressure accumulator pressure (p_{bl}) is above its minimum pre-charged pressure (p_{bl_min}). When p_f is above the P_{fmin} during the increase PV power supply, the pressure accumulator is enabled for charging within the defined pressure limits of the pressure accumulator: minimum p_{bl_min} and maximum set charging limit p_{bl_set}. The control algorithm for enabling this strategic is summarised in Fig. 4.

The set minimum pressure threshold is experimentally determined through a series of steady-state tests of the PV-membrane system at different pressure setpoint.

2.2.3. Pump's maximum ramp-rate threshold test for shutdown control

The maximum PV power ramp-down that can trigger a shutdown of the chosen pump (rr_{pump_max}) is investigated across different pump pressure setpoints. Using the Eq. (1), the identified threshold is furthermore implemented to control shutdowns in the system. If the ramp-down rate exceeds a critical threshold, an impending system shutdown becomes unavoidable. The detailed analysis of PV power ramp-down events leading to system shutdowns for the selected pump are presented in the results section.

3. Experimental investigations

In this study, two types of experiments were conducted: i) steady-state tests and ii) solar day tests. The steady-state tests involve using a fixed power supply to drive the system, while performance is evaluated under different variations. The solar day tests, on the other hand, use real solar days with varying SI conditions to drive the system, allowing for an investigation of its real-world performance. For both experiments, two membranes with distinct desalination characteristics commonly employed in PV-membrane desalination systems were used for the investigation – BW30 and NF90. These membranes were selected to evaluate their performance and response to shutdown control under varying operational conditions.

3.1. Operating setpoints and thresholds experiments

3.1.1. PV-membrane operating thresholds

The operating thresholds of PV-membrane system were investigated over a range of different pressure setpoints from 2 to 12 bar (1 bar increments), to determine the limit at which the performance of the PV-membrane system begins to deteriorate. These tests were conducted under steady-state conditions, where the system operates at a constant feed pressure, flow rate, and/or recovery rate. During these tests, the PV power consumption of the pump was regulated by adjusting the system's back pressure using an actuator valve. This enables the desired pressure setpoints to be realised (i.e., the set maximum pressure for water flow

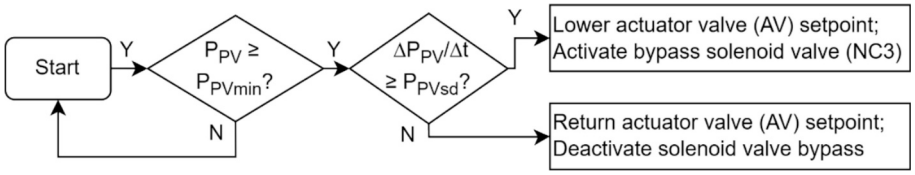

Fig. 3. Control algorithm flowchart of the electrical actuator valve (AV), and bypass solenoid valve NC3.

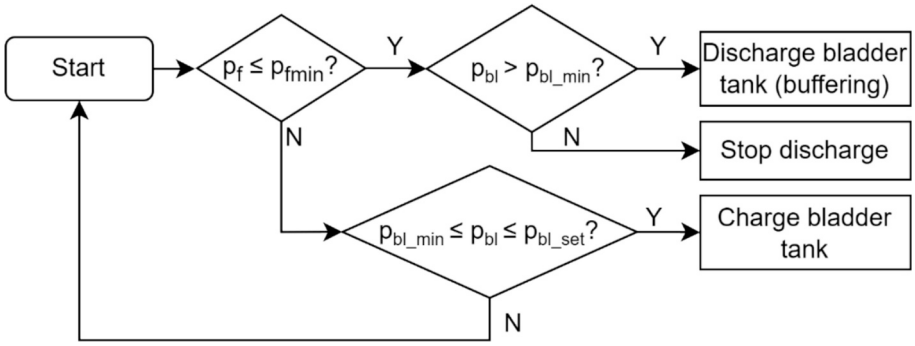

Fig. 4. Control algorithm flowchart of pressure accumulator hydraulic buffering.

through the membranes). These thresholds are subsequently used in control strategies to manage shutdowns in the system The performance of the system was indicated by the metrics of: i) the specific energy consumption (SEC) of ≥5 Wh/L for the BW30 membrane [32] or ≥ 2.5 Wh/L [67] for the NF90 membrane, and ii) permeate production quality exceeding the World Health Organization (WHO)-recommended palatable limit of 0.6 g/L total dissolved solids (TDS), equivalent to 1.133 mS/cm electrical conductivity (EC) [68].

3.1.2. PV power ramp-rate thresholds

This experiment determines the PV power ramp-rate threshold that triggers the pump's shutdown. The test involves varying the pump's power supply in incremental steps per second while maintaining a constant operating pressure setpoint. The power ramp-rate is varied and repeated at different intervals until the pump shuts down. To vary the ramp-rate, a SAS is used to supply a constant power supply, with the supplied current is varied at intervals to achieve a ramp-down. If a ramp-down does not result in a shutdown, the initial power is restored, and the current reduction is increased. This process is repeated until the shutdown occurs.

3.1.3. Pressure accumulator charge-discharge thresholds

This experiment aims to determine the amount of mechanical energy that can be stored in the pressure accumulator and how this also depends on the feed pump's maximum head. When no subsequent recharge is possible after a discharge, the maximum buffering duration of the pressure accumulator is also be identified through this test.

3.2. Solar days experiments

3.2.1. Directly-coupled PV-membrane

This test investigates the PV-membrane system performance when coupled directly to PV power supply without additional control or buffering options. The results are used as a baseline of comparison for other controlled or hydraulic buffered PV-membrane system investigated in the study.

3.2.2. Passive hydraulic buffering

In this setup, the pressure accumulator is implemented for buffering without active control. This means, the inlet and the outlet channels of the pressure accumulator remain open, allowing the feed pump to simultaneously charge the accumulator to the feed pressure while also supplying pressure to the membrane system. The experiment is aimed at investigating the system performance under uncontrolled buffering condition, comparing it to other methods of shutdown control.

3.2.3. Controlled hydraulic buffering

In this setup, the pressure accumulator is pre-charged to the pump head of 12 bar and used for direct pressure buffering using the control logic presented in Fig. 4. The control algorithm manages the charging and discharging of the tank, aiming to minimise continuous charging typically observed in passive buffering. Continuous charging can lower the feed pressure supplied by the pump for desalination, leading to a reduction in daily production capacity. The results are compared to other methods of shutdown control.

3.2.4. Electrical actuated valve control with EHCS for reducing system shutdown

This setup consists of the proposed EHCS which incorporates an electrically-controlled actuator valve to reduce the pressure and consequently the power demand by the pump to prevent shutdown, based on the control algorithm in Fig. 3. Thus, this experiment examines how the valve prevents or minimizes electrical and hydraulic shutdowns in the absence of integrated buffering.

3.2.5. Controlled hydraulic buffering with controlled actuator valve

This experiment combines controlled hydraulic buffering with an electrically actuated valve to analyse their combined impact on overall system performance. Real-time system parameters are monitored to assess how this integrated approach enhances stability and efficiency, offering further insights into improving PV-membrane system reliability.

3.2.6. Short-term analysis of PV power ramp-down with/out controlled actuator valve

This experiment investigates the short-term (< 5 min) impact of pump shutdowns caused by PV power ramp-down events on the performance of the PV-membrane system. This investigation compares the performance of a directly-coupled system during a shutdown to the system when a controlled actuator valve is implemented, and the effectiveness of the valve in mitigating shutdowns can be assessed. Specifically, the experiment checks the controlled valve's ability to reduce the pump's downtime following each shutdown event.

Overall, for the solar day experiments, the directly-coupled PV-membrane system was tested under three solar conditions: Sunny, partly cloudy, and very cloudy days, as introduced in Section 2.1.1*(b)*. Other investigations aimed at controlling both electrical and hydraulic shutdowns were conducted specifically on partly cloudy and very cloudy days. These conditions were selected because the buffering strategies are designed to address fluctuations in PV power supply, which are more pronounced under partly cloudy and very cloudy conditions.

4. Results and discussion

4.1. Steady-state results

4.1.1. PV-membrane steady-state test

Steady-state tests were conducted at various pump operating pressure setpoints, ranging from 2 to 12 bar in 1 bar increments. The parameters investigated include the pump's power demand, SEC, flow rate,

flux, EC rejection, and recovery. The results at these different pressure setpoints for the two investigated membranes are presented in Fig. 5.

The results show that, the system performance begins to improve at a feed pressure of ≥8 bar, with the SEC <5.0 Wh/L for the BW30 membrane (Fig. 5a) and < 2.5 Wh/L for the NF90 membrane (Fig. 5e). While the SEC for both membranes can be further reduced, this pressure serves as the minimum threshold for subsequent control optimization processes. Although the feed flow rate is about the same for both membranes across different pressure setpoints, the permeate flow rate and corresponding flux of BW30 (Fig. 5b) are approximately half of those of NF90 (Fig. 5f). This can be attributed to the permeability of each membrane, with NF membrane having a higher permeability than RO membrane. An increase in permeate flow also leads to a reduction in concentrate flow, maintaining the hydraulic flow balance through the membranes.

The BW30 membrane requires a higher pressure to produce a drinkable permeate (<1.33 mS/cm WHO palatable limit), here realised from 6 bar (Fig. 5c), when the pressure setpoint is at 12 bar. The NF90 membrane realised this at 5 bar (Fig. 5g). It is important to note that when the setpoint is reduced below 12 bar, the membranes would require higher power supply and increased feed pressure to achieve the same permeate quality. BW30 membrane meanwhile demonstrates a higher salt rejection at low pressure (Fig. 5d) compared to NF90 (Fig. 5h).

One observation from this comparison is that while the hydraulic performance of each membrane varies within the operating setpoints, the electrical characteristics are similar irrespective of the membrane. This means, similar power consumption is needed to produce the same pressure comparable for each membrane. This investigation not only helps to identify the pressure threshold for optimization experiments, but also highlights the suitability of the two membranes for specific applications. Overall, the NF90 membrane is more suited for brackish water desalination due to its lower SEC and higher flux, while maintaining acceptable water quality levels. In contrast, BW30 is generally used for more concentrated solutions.

4.1.2. PV power ramp-rate test, and pump maximum shutdown threshold

The PV power ramp-rate was investigated over a pressure setpoint ranging from 2 to 12 bar. This range was chosen based on the maximum head of 12 bar, and the minimum pressure of 2 bar achievable when the PV-membrane valve is fully open. The PV power supply was supplied by the SAS. With the SAS operating in a constant DC power mode, a voltage

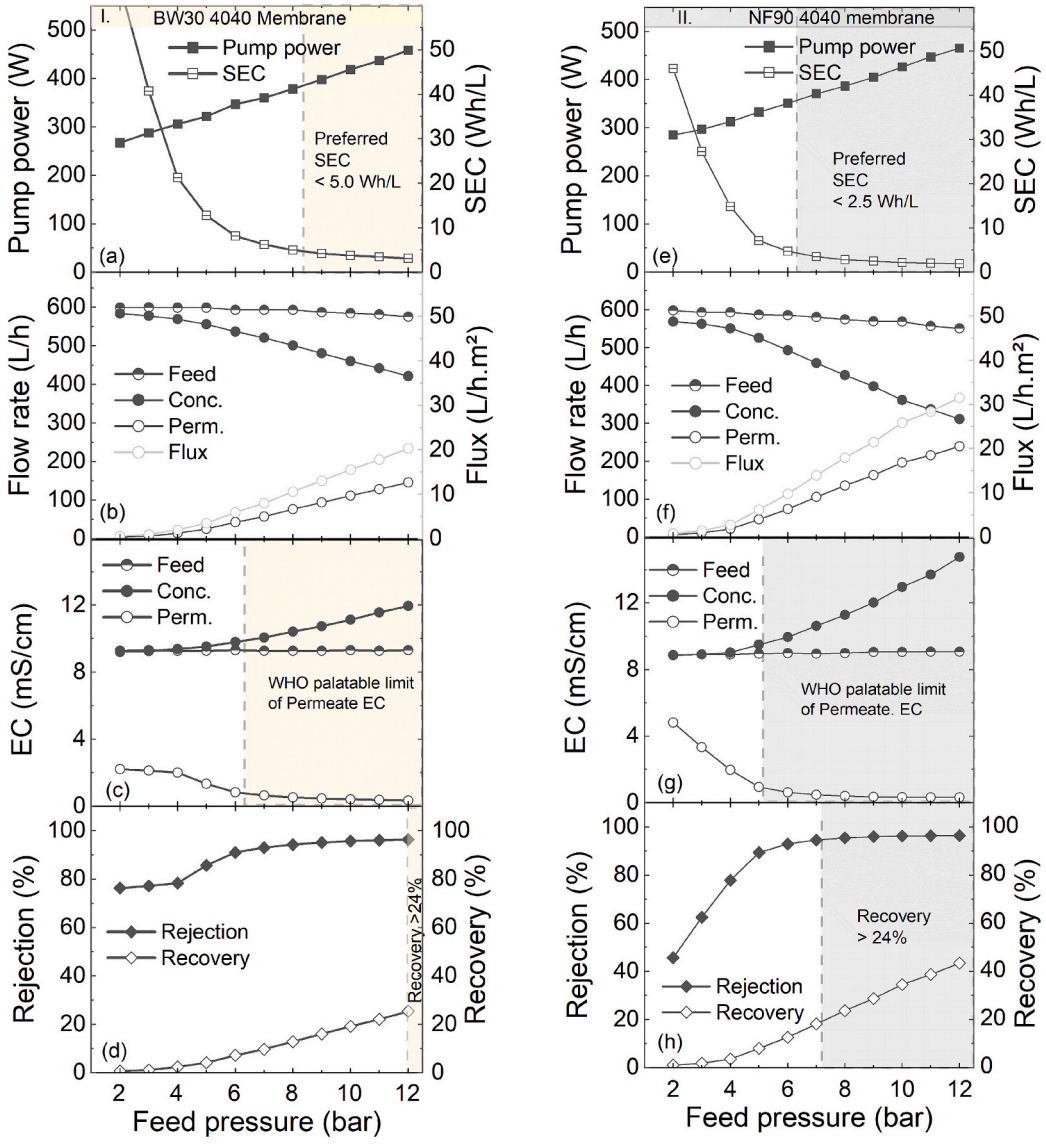

Fig. 5. Steady-state threshold tests of PV-membrane system with I. BW30 (a) Pump power & SEC, (b) Flow rate & flux (c) EC, (d) Salt rejection / water recovery; and II. NF90 (e) Pump power & SEC, (f) Flow rate & flux (g) EC, (h) Salt rejection / water recovery.

of 100 V was set, while the current reduced per second starting at 5 A with an initial reduction rate of 0.1 A /s. If no shutdown occurred at 4.9 A, the maximum current of 5 A was restored, and the reduction rate was increased to 0.2 A / s, ramping down to 4.8 A. This cycle was repeated, incrementally increasing the reduction rate, until a shutdown was induced. The PV power threshold required to cause a shutdown at each operating setpoint was recorded, and the results are summarised in Table II.

The maximum relative PV power deviation that resulted in a shutdown was calculated following the defined parameters in Eq. (1), as the relative difference between the shutdown power deviation from Table II (col. 5 = col. 2 – col. 3) with respect to the initial PV power (col. 2). Similarly, the maximum relative pressure deviation was calculated as the relative difference between the initial setpoint pressure and the pressure at shutdown (col. 1 – col. 4), with respect to col. 1.

The highlight from Table II is that, the maximum relative PV power deviation that is capable of triggering a shutdown of the selected pump is approximately **30 %/s** across different pressure setpoints at any given time during operation. This provides more insights into the control of pump's shutdown in the system, as relying solely on PV power ramp rate per second (W/s) – as employed in other works (such as [69]) – may not be stable across different levels of SI fluctuations levels. It is worth noting that this threshold may differ across different pumps, thus similar ramp-down analysis may be performed to identify the pump's specific ramp-down deviation threshold that can lead to a shutdown. Meanwhile, for experimental work, a **10 %/s** relative deviation was set as the setpoint (Fig. 2), enabling faster system response to open the valve before fluctuations reach the critical 30 %/s peak, towards preventing the shutdown.

4.1.3. Hydraulic energy storage estimation

The hydraulic energy stored in the pressure accumulator and the maximum possible buffering period are determined by investigating the charge-discharge cycle of the tank. The pressure accumulator tank stopped charging when the charged pressure reached the pump's maximum head of approximately 12.2 bar. By integrating the accumulator's feed flow rate defined as F1-F2 in Fig. 1, the volume of water stored in the tank was determined. These parameters – feed pressure (bar) from the pump and charged volume (L) where converted to potential work done (units: Joules [P(bar) × V(L) × 100] to estimate the nominal hydraulic energy stored in the tank, without considering the adiabatic process of pre-charged gas on the stored water. The adiabatic method of estimating the hydraulic energy of the pressure accumulator is presented in the Supplementary Information Section **S2.** The equivalent hydraulic energy supplied by the pump is estimated by multiplying the pump's maximum power consumption (W) at the fixed setpoint, by the charging duration (seconds). The charging time is determined by dividing the charged volume of the pressure accumulator (L) by the differential flow rate (L/min) supplied to it. This approach accounts for the fact that the feed pump was simultaneously supplying the membrane system. The buffering time is defined as the duration for which the pressure accumulator discharges while maintaining a fixed pressure setpoint of 12 bar in the PV-membrane system. The charged and discharged characteristics of the accumulator are presented in Table III and summarised in **Fig. S1** of the Supplementary Information.

The highlights of this investigation are: i) The energy stored in pressure accumulator as well as its buffering time, are very limited to sustain continuous buffering process. These can only be replenished if the pump operates continuously to recharge the system. ii) The maximum round-trip efficiency of the pressure accumulator. The maximum round-trip efficiency of the pressure accumulator is relatively low, approximately 44 %, while the pump's maximum efficiency reaches about 47 % [50] at its maximum head. The round-trip efficiency is calculated as the ratio of the hydraulic energy delivered by the accumulator to the electrical energy supplied to the pump for generating the charging pressure. This low efficiency is primarily due to the losses during the pump's conversion of electrical energy into hydraulic energy. As a pressure accumulator stores pressure directly without additional energy conversion during buffering, the overall round-trip efficiency is thus predominantly constrained by the efficiency of the electrical pump used in the system.

4.2. Solar days results

This study considers three types of solar days: Sunny, partly cloudy, and very cloudy. The sunny day exhibits negligible SI fluctuations, resulting in no system shutdowns. As such, the sunny day served as a reference for assessing the PV-membrane system's performance under clear sky conditions, with results presented in Supplementary Information Section **S3.** The focus on shutdown management was directed towards partly cloudy and very cloudy days, where significant PV power fluctuations occur. These conditions were addressed using hydraulic buffering and actuator valve control strategies with EHCS.

This section details the experimental results of these control strategies on PV-membrane system. Experiments were performed using two types of membranes (BW30 and NF90) to identify the most effective method for managing shutdowns across different desalination membrane technologies.

4.2.1. Partly cloudy and very cloudy days test with BW30 membrane

The results of the hydraulic buffering and control with actuator valve when tested on a partly cloudy day as well as very cloudy day using BW30 membrane are presented in Figs. 6 and 7, while the summary of the average daily performance parameters is provided in Table IV.

The pump's electrical shutdown is identified when its power consumption drops to zero. Figs. 6 **(a, f, k, p)** and **7 (a, f, k, p)** depict the electrical shutdown events observed under different configurations: directly coupled, passive buffering, controlled buffering, and actuator valve control, on partly cloudy and very cloudy days, respectively. The data shows that during the discharge phase of the pressure accumulator

Table II
PV power ramp-down maximum threshold for pump shutdown (referenced to **Eq. 1**).

Setpoint pressure (bar)	Initial PV power P_t (W)	PV power supply at pump's shutdown $P_{(t-\Delta t)}$ (W)	Pressure at shutdown (bar)	Shutdown power deviation $P_t - P_{(t-\Delta t)}$ (W)	Max. relative PV power deviation ΔP_{PVrel} (%/s)	Max. relative pressure deviation (%/s)
12	459	309	8.4	150	32.7	30.0
11	439	297	7.9	142	32.4	28.2
10	421	285	7.1	136	32.3	29.0
9	403	283	6.5	120	29.8	27.8
8	381	276	5.8	106	27.8	27.5
7	366	263	5.0	103	28.1	28.6
6	344	251	4.2	93	27.0	30.0
5	329	238	3.5	92	28.0	30.0
4	313	214	2.7	99	31.6	32.5
3	296	202	2.0	95	32.1	33.3
2	278	189	0	89	32.0	–
				Average	30.4	29.7

Table III
Pressure accumulator charge-discharge performance tests at different charged pressure.

Pump			Pressure accumulator					
Power at max. Pressure (W)	Charging time (ss)	Estimated Energy supply (Wh)	Charged pressure (bar)	Charged volume (L)	Discharge (buffering) time (mm:ss)	Hydraulic energy supply (J)	Hydraulic energy supply (Wh)	Round-trip efficiency (%)
459	83	10.6	12.2	13.8	03:35	16,836	4.7	44.2
459	77	9.8	11.0	12.7	02:54	13,970	3.9	39.5
459	71	9.1	10.0	11.8	02:42	11,800	3.3	36.2
459	64	8.2	9.0	10.6	02:33	9540	2.7	32.5
459	58	7.4	8.0	9.3	02:18	7440	2.1	27.9
459	46	5.9	7.0	7.6	01:52	5320	1.5	25.2
459	34	4.3	6.0	5.6	01:36	3360	0.9	21.5
459	16	2.0	*5.0	2.6	01:01	1300	0.4	17.7

* The pressure accumulator is pre-charged to 4 bar with air, thus when the pump's feed pressure ≤ 4 bar, there is no charge stored in the accumulator.

(in passive buffering and controlled buffering), there was an increased electrical shutdown of the pump. This is due to an increased pressure resistance in the feed flow line during the hydraulic buffering which must be overcome by the feed pump's pressure. During PV power ramp-down events, if the pump cannot generate sufficient pressure to overcome the buffering resistance from the pressure accumulator, it shuts down.

Meanwhile, it is worth noting that while the actuator valve control method with the ECHS may cause multiple temporary drops in permeate flow rate throughout the day, these are momentary responses lasting only about 1 s each time the actuator bypass is triggered to reduce pressure. These brief interruptions thus have a very minimal impact on daily production, unlike a pump shutdown, which results in a significant dead time. With the selected pump, each pump shutdown could result in a downtime of up to 30 s before the pump's electronics makes an attempt to restart.

The electrical actuator valve configuration with the EHCS successfully minimised electrical shutdowns in the system, utilising the

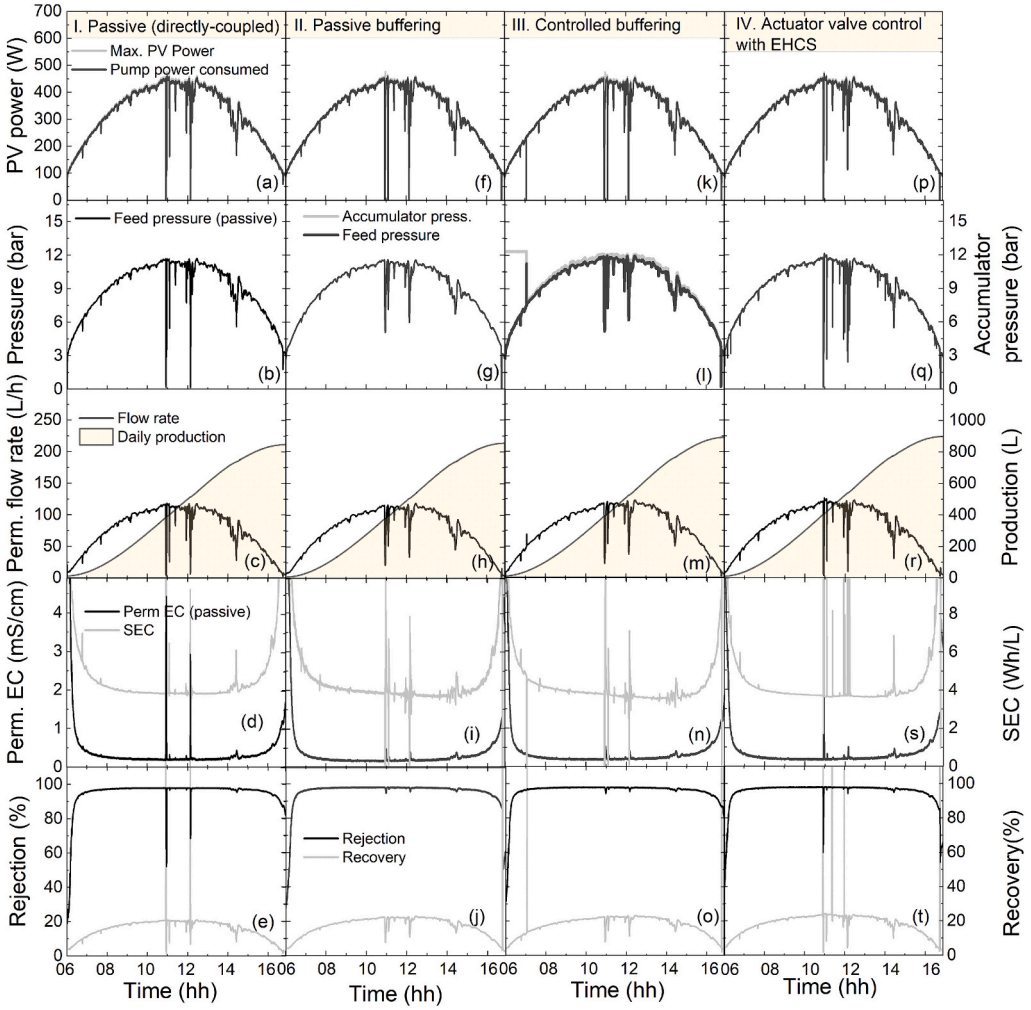

Fig. 6. PV-membrane system performance with different operational methods on a partly cloudy day with BW30 membrane. I. Directly-coupled configuration II. Passive buffering, III. Controlled buffering IV. Controlled actuator valve with EHCS: (a,f,k,p) PV power supply and consumption; (b,g,i,q) Feed pressure and accumulator's charged pressure; (c,h,m,r) Flow rates and daily production; (d,i,n,s) Permeate EC and SEC; (e,j,o,t) Rejection and recovery.

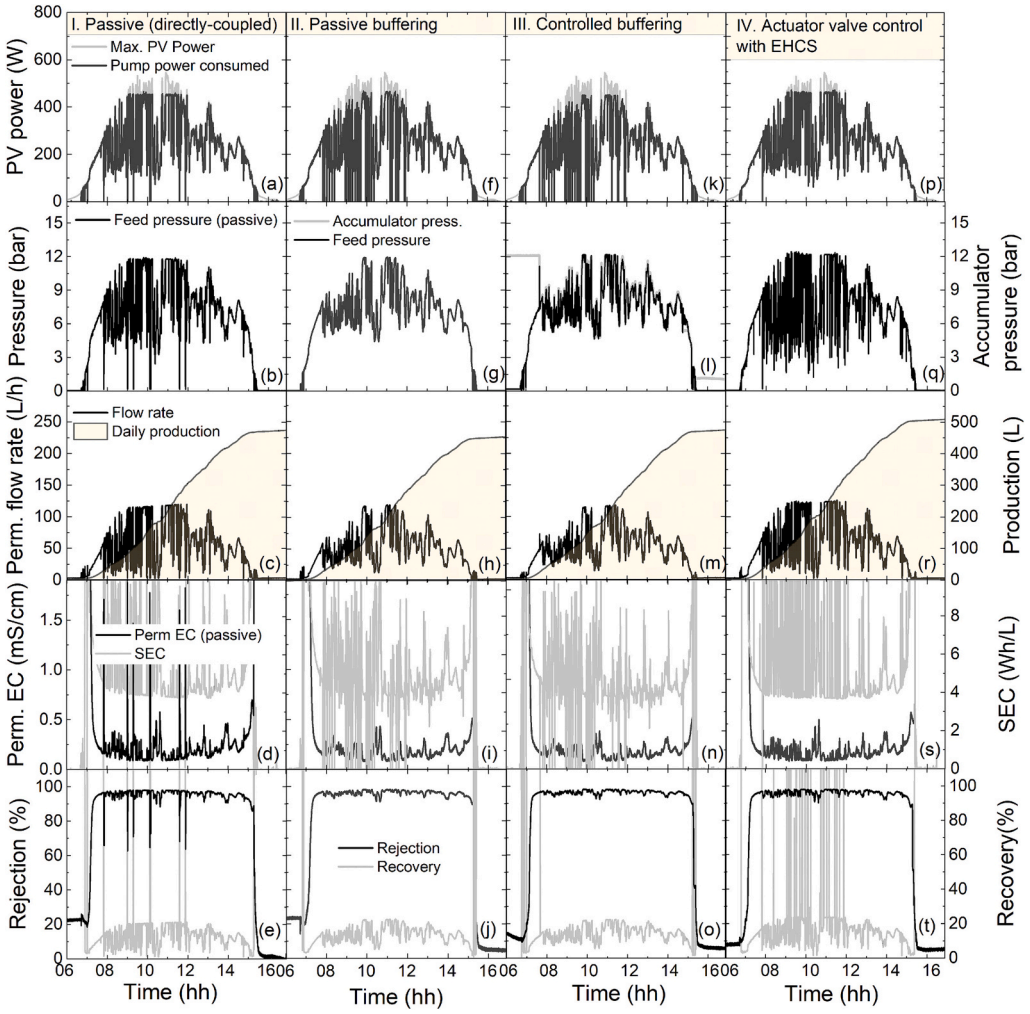

Fig. 7. PV-membrane system performance with different operational methods on a very cloudy day with BW30 membrane. I. Directly-coupled configuration II. Passive buffering, III. Controlled buffering IV. Controlled actuator valve with EHCS: (a,f,k,p) PV power supply and consumption; (b,g,i,q) Feed pressure and accumulator's charged pressure; (c,h,m,r) Flow rates and daily production; (d,i,n,s) Permeate EC and SEC; (e,j,o,t) Rejection and recovery.

Table IV
Average daily performance of PV-membrane system with BW30 across different configurations and control methods.

Solar days	System performance (BW30)	System configurations				
		Reference: Passive (directly coupled)	Passive hydraulic buffering	Controlled hydraulic buffering	EHCS	Controlled buffering + EHCS
Partly cloudy	# pump shutdowns	2	4	5	1	1
	Daily production (L)	848	85↑ (1.0 %)	892	899↑ (1.0	877
	(% change c.f. ref.)	–		↑ (1.0 %)	%)	↑ (1.0 %)
	Avg. EC (μS/cm)	369	405	342	389	417
	Avg. SEC (Wh/L)	5. 0	4.8	4.5	4.8	4.7
	Rejection	96.0	95.5	96.3	95.7	95.4
	Recovery	16.1	18.2	18.1	19.4	18.8
Very cloudy	# pump shutdowns	7	36	32	1	20
	Daily production (L)	468	447	469	503	475
	(% change c.f. ref.)	–	↓ (−4.5 %)	↑(0.2 %)	↑(7.5 %)	↑(1.5 %)
	Avg. EC (μS/cm)	781	736	714	676	723
	Avg. SEC (Wh/L)	6.0	5.4	5.0	6.2	5.9
	Rejection (%)	91.5	91.8	92.2	92.5	91.9
	Recovery (%)	21.3	19.1	17.7	22.1	18.8

proposed algorithm and valve bypass method. This approach effectively manages fluctuations in PV power supply, preventing shutdowns by dynamically adjusting valve positions and controlling pressure. Figs. 6 (b, g, l, q) and 7 (b, g, l, q) illustrate the variations in feed pressure and accumulator pressure across four configurations: directly coupled, passive buffering, controlled buffering, and controlled actuator valve-only methods. During low power supply or rapid PV power ramp-down events, the pressure accumulator's discharge provides hydraulic buffering (Figs. 6 and 7g,l) to mitigate SI fluctuations. This however increases the electrical shutdowns of the pump. With the implementation of the controlled actuator valve (Figs. 6q and 7q), electrical shutdowns were significantly minimised, thereby also preventing corresponding

hydraulic shutdowns.

Figs. 6 (c, h, m, r) and 7 (c, h, m, r) present the daily flow rate and production observed respectively on partly cloudy and very cloudy days across the four configurations: directly coupled, passive buffering, controlled buffering, and actuator valve-controlled methods. The actuator valve-controlled configuration consistently exhibited slightly higher daily production compared to the other configurations. This improvement is attributed to the significant reduction in pump shutdown events. Each time the pump shuts down, it requires a dead time of over 30 s for the electronics to reactivate after the shutdown event. By minimising these shutdowns, the actuator valve control method with EHCS eliminates such downtime, thereby enhancing overall production efficiency.

Multiple electrical shutdowns of the pump can lead to increased SEC and higher permeate EC as evident in Figs. 5 (d, i, n, s) and 6 (d, i, n, s), where the configurations experiencing frequent pump shutdowns show higher daily averages for EC and SEC. Meanwhile, the actuator valve control method minimizes pump shutdowns and enhances daily production, however, the average SEC for this method appears higher compared to other configurations. This is because, when the actuator and bypass valves briefly open to relieve back pressure and prevent shutdowns, the concentrate flow momentarily increases due to the bypass. This causes the permeate flow to drop nearly to zero (~0 L/h) for a very short time (e.g.1 s) to balance the flow dynamics. Since SEC is calculated as power supply (W) divided by permeate flow rate (L/h), these brief drops result in occasional SEC spikes. The average daily SEC in Table IV however does not reflect the operational energy efficiency of the system, as evidenced by the stable average daily permeate EC and increased daily production.

On the partly cloudy day (Fig. 6 e, j, o, t), the average rejection was relatively consistent at about 96 %, while on the very cloudy day (Fig. 7 e, j, o, t), it was approximately 92 %. On both days, the actuator valve control method enabled a slightly higher average recovery rate compared to the other configurations which indicates the possibility of valve-controlled system helping to realize an enhanced daily production under less favourable SI conditions with BW30 membrane.

The final configuration, which combined controlled buffering with the actuator valve control (with EHCS), showed only limited improvement over the directly-coupled system. This suggests that the drawbacks associated with increased electrical shutdowns during hydraulic buffering offset the potential benefits of the combined approach. As a result, the hybrid of these two strategies did not yield better performance in this experiment. This limitation will be addressed in future studies. The full results of this investigation can be found in Supplementary Information **S4.**

4.2.2. *Partly cloudy and very cloudy days test with NF90 membrane*

The hydraulic buffering and actuator valve control configurations where also tested on a partly cloudy day and a very cloudy day using NF90 membrane. The results are presented in Figs. 8 and 9, while the

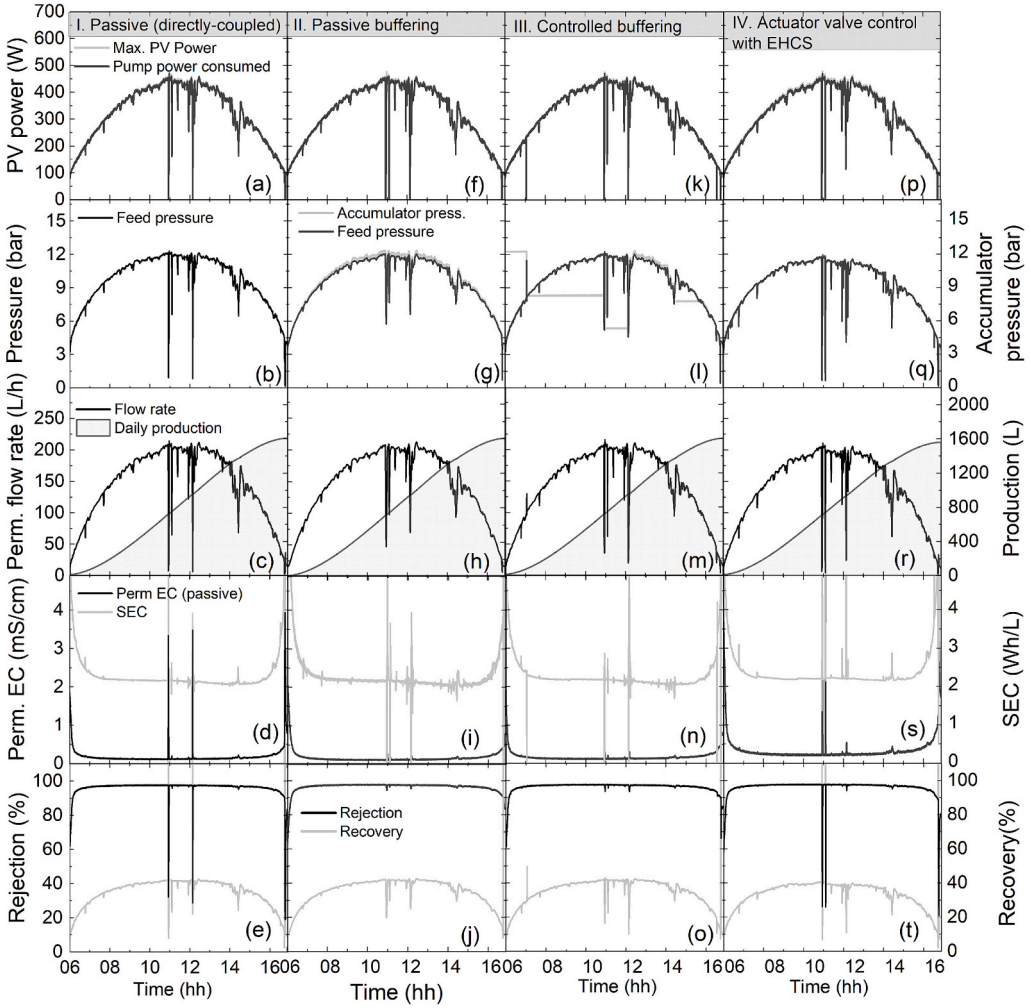

Fig. 8. PV-membrane system performance with different operational methods for NF90 on a partly cloudy day. I. Directly-coupled configuration II. Passive buffering, III. Controlled buffering IV. Actuator valve control (with EHCS): (a,f,k,p) PV power supply and consumption; (b,g,i,q) Feed pressure and pressure accumulator pressure; (c,h,m,r) Flow rates and daily production; (d,i,n,s) Permeate EC and SEC; (e,j,o,t) Rejection and recovery.

summary of the average daily performance parameters is provided in Table V. The pump's electrical shutdown behaviour was investigated using the NF90 membrane under various configurations, as shown in Figs. 8 (a, f, k, p) and 9 (a, f, k, p) for partly cloudy and very cloudy days, respectively. Similar to the BW30 membrane, there was an increase in electrical shutdown events during the hydraulic buffering period with the pressure accumulator, particularly during SI fluctuations. However, the actuator valve control effectively minimised pump shutdowns during these periods, as summarised in Table V. Notably, the valve control method demonstrated greater effectiveness during conditions with frequent ramp-down events, such as on very cloudy days, compared to partly cloudy days, which experienced only two major ramp-down events.

As likewise emphasized for BW30 membrane operations, the high number of permeate flow rate approaching zeros occurred as momentary responses lasting only about 1 s each time the actuator bypass is triggered to reduce pressure. This however has no major negative effect over the total daily production on a very cloudy day with multiples pump shutdowns.

The hydraulic variations observed with the pressure accumulator buffering and valve control methods, illustrated in Figs. 8 (b, g, l, q) and 9 (b, g, l, q) for partly cloudy and very cloudy days, respectively, highlighted the ability of the pressure accumulator to maintain steady hydraulic feed and permeate flow. Despite this advantage, the pressure accumulator's operation was accompanied by an increased occurrence of electrical shutdowns in a similar way as realised with the BW30 membrane system.

When comparing daily production for both partly cloudy (Fig. 8 c, h, m, r) and very cloudy (Fig. 9 c, h, m, r) solar days, the controlled valve configuration shows minimal or no major improvement on the partly cloudy day. This is because only one major shutdown was prevented, resulting in limited production gain. Mainly, the momentary triggering of the valve and bypass reduces permeate flow rate during operation. However, on very cloudy days with frequent fluctuations, valve control is significantly more effective, as production gains are primarily achieved by eliminating the pump's dead time following shutdowns.

Electrical shutdowns across all investigated configurations meanwhile leads to increased SEC and permeate EC values on both partly cloudy (Fig. 8 d, i, n, s) and very cloudy (Fig. 9 d, i, n, s) solar days. However, the valve control method demonstrated superior performance on the very cloudy day, achieving an average SEC of 2.4 Wh/L and an EC of 501 μS/cm, which were significantly better than those of other configurations. This highlights the effectiveness of valve control in maintaining system efficiency and water quality under challenging SI conditions.

Fig.s 8 (e, j, o, t) and 9 (e, j, o, t) illustrate the rejection and recovery rates across the investigated configurations for partly cloudy and very cloudy days, respectively. The average performance of the configurations is generally comparable, except for the directly coupled (Figs. 8e and 9e) and valve-controlled (Figs. 8t and 9t) setups, which exhibit

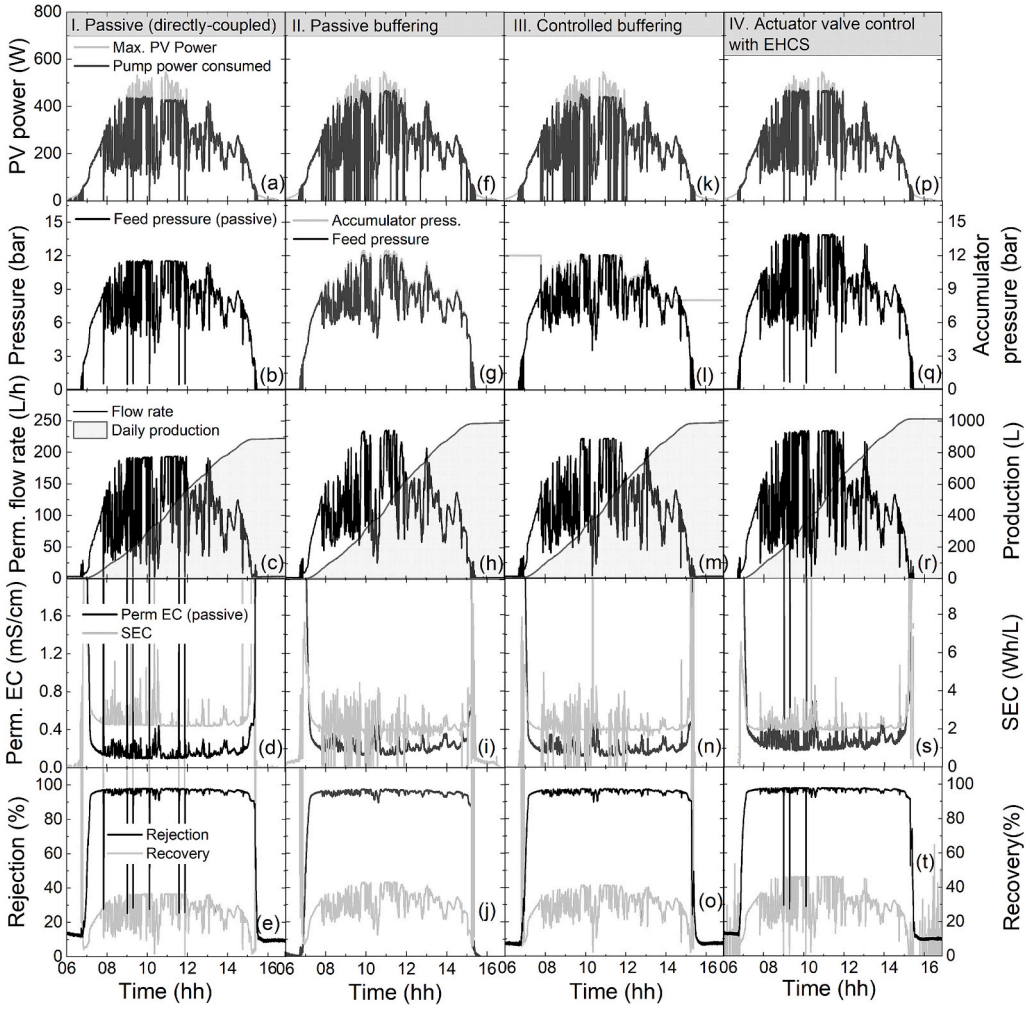

Fig. 9. PV-membrane system performance with different operational methods for NF90 on a very cloudy day. I. Directly-coupled configuration II. Passive buffering, III. Controlled buffering IV. Controlled valve only. (a,f,k,p) PV power supply and consumption; (b,g,i,q) Feed pressure and pressure accumulator pressure; (c,h,m,r) Flow rates and daily production; (d,i,n,s) Permeate EC and SEC; (e,j,o,t) Rejection and recovery.

Table V
Average daily performance of PV-membrane with NF90 across different configurations and control methods.

Solar days	System performance (NF90)	System configurations				
		Reference Passive (directly coupled)	Passive hydraulic buffering	Controlled hydraulic buffering	EHCS	Controlled buffering + EHCS
Partly cloudy	# pump shutdowns*	2	2	2	2	5
	Daily production	1615	1613↓	1611 ↓	1567↓	1507 ↓
	(% change c.f. ref.)	–	(−1.0 %)	(−1.0 %)	(−1.0 %)	(−0.9 %)
	Avg. EC (μS/cm)	355	327	322	365	364
	Avg. SEC (Wh/L)	2.4	2.3	2.4	2.6	2.6
	Rejection	96.1	96.4	96.4	96.0	96.0
	Recovery	36.5	35.8	35.2	34.1	32.5
Very cloudy	# pump shutdowns*	7	36	33	3	15
	Daily production (L)	884	981↑	983↑	1013↑	831↓
	(% change c.f. ref.)	–	(11.0 %)	(11.0 %)	(14.6 %)	(−6.0 %)
	Avg. EC (μS/cm)	629	794	648	501	658
	Avg. SEC (Wh/L)	2.9	2.3	2.3	2.4	3.2
	Rejection (%)	93.1	91.3	92.9	94.5	92.7
	Recovery (%)	28.2	33.5	33.9	29.7	34.1

spikes in rejection corresponding to periods of the pump's electrical shutdowns.

The complete performance parameters, including these variations, are summarised in Table V for further comparison and analysis. The hybrid configuration of both controlled buffering with the actuator valve control (with EHCS), showed only limited improvement over the directly-coupled system. The full results of this investigation can be found in the Supplementary Information Section S5.

4.2.3. Summary of system performance and shutdown control

The summary of the key performance indicators (average daily EC, specific, average daily SEC, daily water production and number of system shutdowns) which are already reported in Tables IV and V are graphically presented in Fig. 10 and Fig. 11.

The conditions of SI or solar days influence the average daily permeate EC with lower production quality observed on very cloudy days (Fig. 10 a,d). However, EHCS maintained the lowest permeate EC across both membrane types under very cloudy conditions. On a partly cloudy day, which has a minimal fluctuation (about 2 per day), the EHCS had a negligible effect on system performance. The average daily permeate EC indicates that EHCS performs better with NF90 membranes and no significant improvement compared to the other configurations when using BW30 membranes. The average daily SEC **(**Fig. 10b, e**)** shows that the EHCS has a slightly higher SEC than the directly-coupled BW30 on a very cloudy day, but the SEC is lower when using NF90. The theoretically high SEC value arise because SEC is calculated as power divided by permeate flow rate. During each concentrate flow bypass event in the EHCS to prevents shutdown, the permeate flow momentarily drops (~1 s), causing a temporary spike in calculated SEC. However, in practice, the EHCS is more efficient, as it achieves higher overall daily water production with the same power supply compared to other methods.

Similarly, daily production on very cloudy days **(**Fig. 10 **c,f)** improved for both membranes when using EHCS. However, on partly cloudy days, the performance of EHCS was only on par with the other configurations. Regarding the system's shutdown, the EHCS also enables the lowest shutdown possible using with respect to different membranes (e.g. from 7 to 1 on a very cloudy day with BW30 and 7 to 3 with NF90 on the same day as shown in Fig.s 11a and Fig. 11b. It should be noted that the difference in performance is primarily attributed to the permeabilities of the membranes. The NF90 membrane, having a higher permeability than the BW30, enables an enhanced daily flux and production, at lower pressure compared to BW30. However, due to its higher porosity, the pressure drop during intermittent pressure bypass was insufficient to fully prevent shutdowns whenever the EHCS was utilised.

These findings highlight the impact of membrane types, having different permeabilities and feed pressure requirements, on the effectiveness of control strategies investigated for shutdowns control in PV-membrane system. The EHCS tries to strike a balance across these configurations, thus effectively minimising the number electrical shutdowns while also enabling an increased daily production especially on a very cloudy day, without relying on additional energy buffering integration.

4.3. Short-term analysis of PV power ramp-down with/out actuator valve control

A short-term (4 min) ramp-down analysis was investigated on a very cloudy day using a BW30 membrane between 11:34 and 11:39 am where one of the major ramp-downs occurred. The aim is to determine how the magnitude of PV power deviation per second causes a shutdown at the threshold ≥30 %/s. The system performance of a directly-coupled system was compared to a actuator valve control method with EHCS. The results are respectively presented in Figs. 12a and 12b with detailed data from the 5 s preceding the shutdown summarised in Table VI for each configuration method.

Fig. 12a, shows that the electric shutdown of the pump was followed by a recovery period of 32 s while there was no pump shutdown with the use of EHCS as shown in Fig. 12b. The data presented in Table VI shows that the shutdowns occurred when the relative PV power ramp-down was above **30 %** which supports the maximum empirical threshold identified as 30 % beyond which an imminent shutdown of the pump becomes unavoidable when uncontrolled.

With the actuator valve control method, although the relative PV power ramp-down above 30 %/s was observed, the pump however did not shut down due to the rightly intervention of the actuated controlled valve, augmented with a bypass valve for fast response. Additional verification of the ramp-rate analysis at different time stamp on a partly cloudy day was done and reported in the Fig. S5 and Table S3 of the Supplementary Information.

5. Conclusion

In this study, two shutdown control strategies are considered for PV-membrane system: i) A novel electrohydraulic control system (EHCS) is designed to strategically control the electrical shutdowns of the pump; ii) a pressure accumulator (bladder tank) was integrated to provide a direct pressure buffering to reduce the hydraulic shutdown of the permeate during the periods of SI fluctuations. Both configurations were tested across different solar days (sunny, partly cloudy and very cloudy days) using different membrane types of different permeabilities: BW30

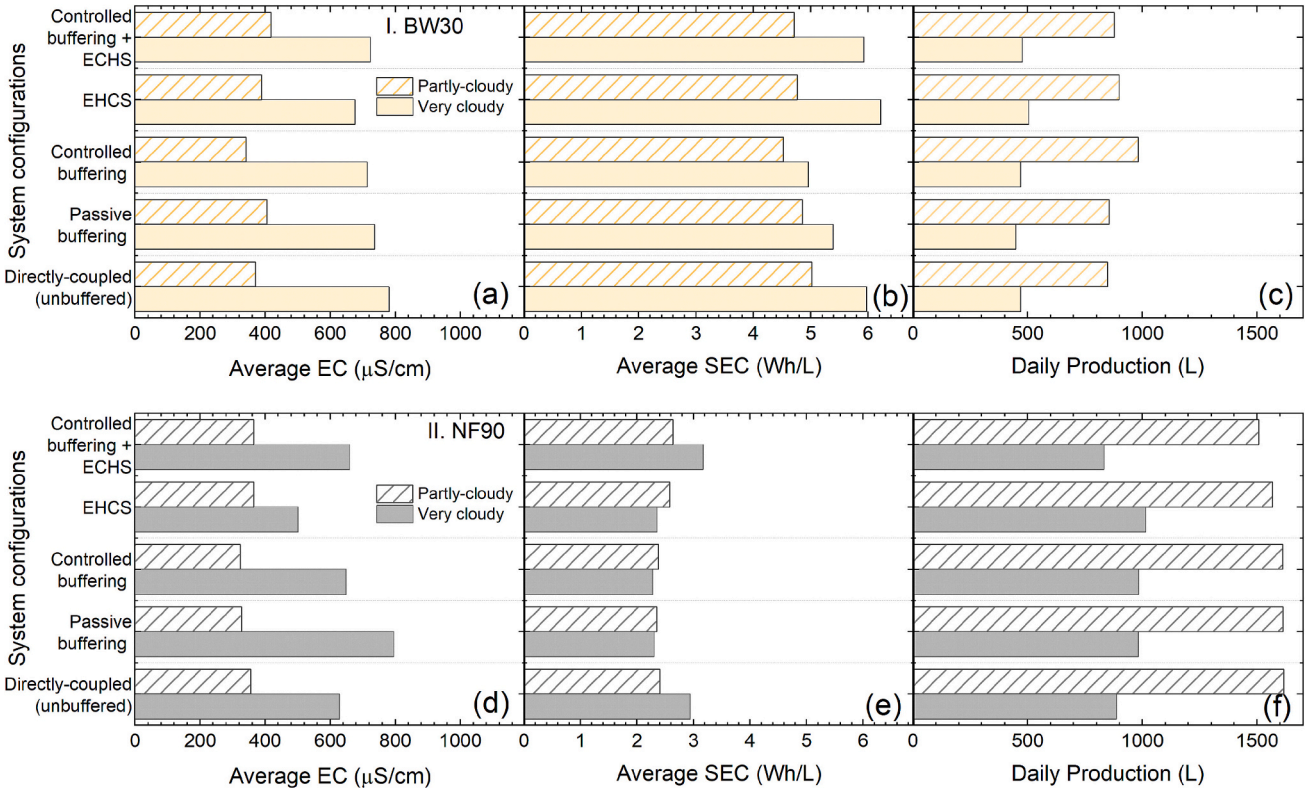

Fig. 10. Average daily system performance and key parameters investigated across different system configuration methods with I. BW30 a) Average EC; b) Average SEC; c) Daily production; II. NF90 d) Average EC; e) Average SEC; f) Daily production.

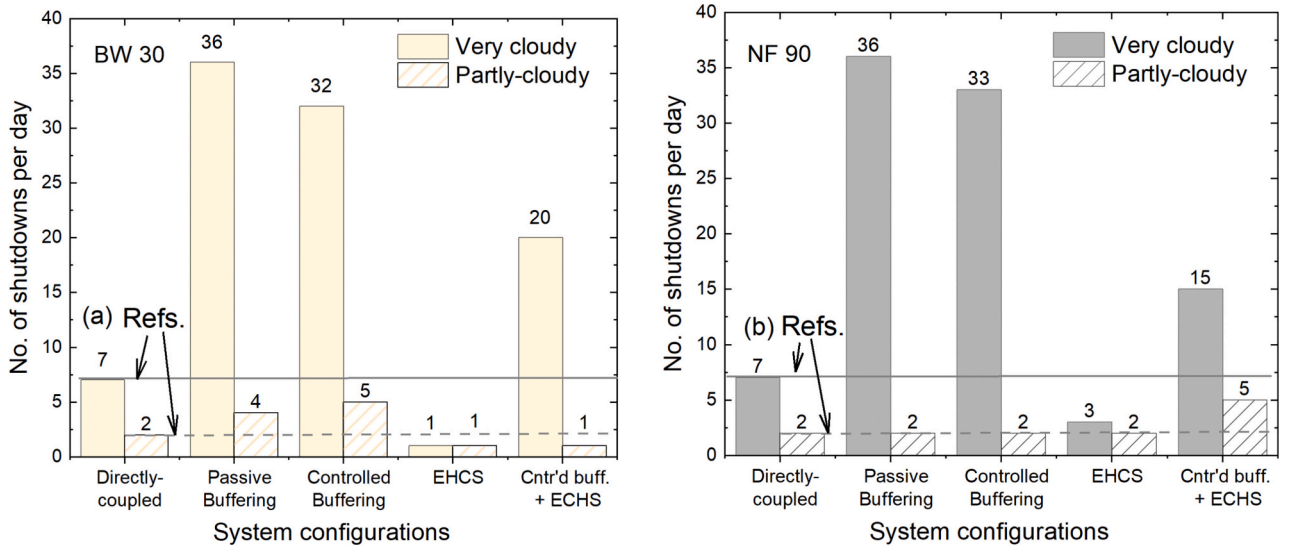

Fig. 11. Average daily shutdowns using different system configurations with (a) BW30 and (b) NF90 membranes. References (Refs.) indicate the number of shutdowns on partly cloudy and very cloudy days using a directly coupled configuration.

reverse osmosis membrane and NF90 membrane. To determine the effectiveness of the configurations on system performance, the following experiments are investigated: i) directly-coupled system (with no EHCS and buffering option) ii) passive buffering with pressure accumulator iii) controlled buffering with pressure accumulator, iv) the proposed EHCS, and v) hybrid configuration of controlled pressure buffering and the EHCS.

The results demonstrate that the EHCS effectively minimise pump electrical shutdowns by rapidly adjusting the operation of an electrically actuated valve in response to PV power ramp-down events during SI fluctuations. This dynamic control simultaneously reduces the hydraulic shutdown of the permeate flow, enabling to an increase in daily water production. On very cloudy days, the EHCS enhanced the daily production by 7.5 % for BW30 and 14.6 % for NF90 compared to directly coupled configurations. On the same day, pump shutdowns were reduced, from seven (7) events to one (1) for BW30 and from seven (7) events to three (3) for NF90. Additionally, the system maintains the water quality within the palatable drinkable water level, at a daily EC

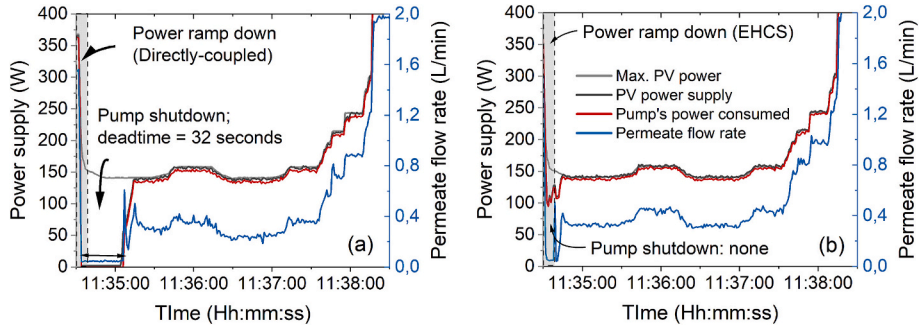

Fig. 12. A short-term (4 mins) PV power shutdown analysis during a ramp-down with a) directly-coupled (passive) configuration and b) actuator valve control with EHCS.

Table VI
A 5-s overview of PV power ramp-rate on system performance. Parameters evaluated follows the previously described parameters in Eq. (1).

Time (hh:mm:ss)	PV power $P_{(t-\Delta t)}$ (W)	PV Power drop (P_t) (W)	Absolute PV power ramp-down (W)	Relative PV power ramp-down ΔP_{PVrel} (%/s)	Pump power (W)	Perm. flow rate (L/min)
Directly-coupled						
11:34:30	367.1	365.5	1.6	0.4	364	1.55
11:34:31	365.5	366.1	0.6	0.2	363	1.55
11:34:32	366.1	235.6	130.5	35.6	362	1.56
11:34:33	235.6	2.2	233.4	99.0	233	0.81
11:34:34	2.2	2.2	0.1	2.3	0	0.04
11:34:35	2.2	2.2	0.0	0.8	0	0.04
Actuator valve control with EHCS						
11:34:30	368.1	275.6	92.5	25.1	363	1.64
11:34:31	275.6	163.5	112.1	40.7	273	0.85
11:34:32	163.5	103.7	59.8	36.6	158	0.10
11:34:33	103.7	98.9	4.8	4.6	100	0.05
11:34:34	98.9	112.0	13.0	13.2	95	0.05
11:34:35	112.0	104.7	7.3	6.5	108	0.04

average of 676 μS/cm and 501 μS/cm for BW30 and NF90 respectively. The daily average SEC of 6 Wh/L was realised for BW30 and 2.4 Wh/L for NF90.

The investigations of direct pressure buffering with a pressure accumulator (either in a passive or controlled configuration) resulted in increased the frequency of pump electrical shutdowns. This is observed to be attributed to the increased positive pressure gradient experienced by the pump during the pressure accumulator's discharge, resulting in high pressure deviations that can trigger the pump shutdowns. Consequently, daily system performance with direct hydraulic buffering was lower compared to either an unbuffered system or the EHCS-integrated configuration.

Regarding membrane selection, a membrane with high permeability like NF90 can meanwhile improve the performance of a PV-membrane system, particularly under low operating pressure, compared to the denser BW30 membrane. However, the high permeability of NF90 poses a challenge for actuator valve control: During intermittent pressure bypass operations of the EHCS, the pressure drop may become inadequate to completely prevent ramp-down effects, potentially leading to shutdowns. On the other hand, the BW30 membrane exhibits reliable shutdown control, especially during very cloudy days with multiple solar irradiance fluctuations.

Overall, this study highlights the ability of the EHCS, employing an electrical actuated valve, to reduce or prevent system shutdowns with optimised performance under unfavorable weather conditions (partly cloudy and very cloudy days). The reduced pump shutdowns due to EHCS directly contributed to increased daily production. For solar conditions with fewer fluctuations, a dynamic control strategy alternating between different hydraulic control methods could further enhance PV-membrane system performance, promoting autonomous and continuous operation across varying SI conditions.

CRediT authorship contribution statement

Emmanuel Ogunniyi: Conceptualization, Methodology, Investigation, Software, Validation, Visualization, Formal analysis, Original draft preparation.

Bryce S. Richards: Conceptualization, Formal analysis, Methodology, Supervision, Resources, Visualization, Writing- Reviewing and Editing, Project administration, Funding acquisition.

Declaration of competing interest

The authors declare that they have no known competing financial interests or personal relationships that could have appeared to influence the work reported in this paper.

Acknowledgements

The authors would like to acknowledge: the PhD scholarship for Emmanuel Ogunniyi provided by the Deutscher Akademischer Austauschdienst (DAAD); Rauna Ndapandula Kasheeta (University of Namibia) for her support during the experimental work and system installation. Bryce Richards gratefully acknowledges funding from the Helmholtz Association via the MTET (Materials and Technologies for the Energy Transition) program – Topic 1 – Photovoltaics (38.01.04), and the professorial recruitment initiative.

Appendix A. Supplementary data

Supplementary data to this article can be found online at https://doi.org/10.1016/j.desal.2025.118784.

Data availability

Data will be made available on request.

References

[1] Worldometer. "Current World Population." https://www.worldometers.info/world-population/ (accessed 22.12.2024).
[2] J.N. O'Sullivan, Demographic delusions: world population growth is exceeding most projections and jeopardising scenarios for sustainable futures, World 4 (3) (2023) 545–568.
[3] UnitedNationsDepartmentofEconomicandSocialAffairs, Prospects 2022: Summary of Results. UNDESA/POP/2022/TR/NO. 3, 2023.

[4] R. Apolinário, R. Castro, Solar-powered desalination as a sustainable long-term solution for the Water scarcity problem: case studies in Portugal, Water 16 (15) (2024) 2140.
[5] S. Kuzma, L. Saccoccia, and M. Chertock. "25 Countries, Housing One-Quarter of the Population, Face Extremely High Water Stress." World Resource Institute (WRI). https://www.wri.org/insights/highest-water-stressed-countries (accessed 22.12.2024).
[6] G. Howard, J. Bartram, A. Williams, A. Overbo, J.-A. Geere, W. H. Organization, Domestic Water Quantity, Service Level and Health, World Health Organization, 2020.
[7] M.B. Danoune, T.R. Ayodele, Techno-economic design of a renewable energy-based reverse osmosis desalination system for an industrial area in Algeria: the case of Adrar's oil refinery, Desalination 601 (2025) 118569.
[8] S.N. Farabi, et al., The future of solar-driven interfacial steam generation for sustainable water desalination: drivers, challenges, and opportunities-review, Results Eng. 23 (2024) 102649.
[9] S. Li, Y.-H. Cai, A.I. Schäfer, B.S. Richards, Renewable energy powered membrane technology: a review of the reliability of photovoltaic-powered membrane system components for brackish water desalination, Appl. Energy 253 (2019) 113524.
[10] U.N.-. Water, Summary Progress Update 2021: SDG 6—Water and Sanitation for all, Geneva, Switzerland (2021).
[11] UnitedNations, Department of Economic and Social Affairs (2016), Indicators of Sustainable Development: Guidelines and Methodologies, United Nations, New York, 2016.
[12] J. Bundschuh, M. Kaczmarczyk, N. Ghaffour, B. Tomaszewska, State-of-the-art of renewable energy sources used in water desalination: present and future prospects, Desalination 508 (2021) 115035.
[13] Y.-H. Cai, Y.-A. Boussouga, A.I. Schäfer, Renewable energy powered membrane technology: impact of intermittency on membrane integrity, Desalination 580 (2024) 117504.
[14] I. Nurjanah, T.-T. Chang, S.-J. You, C.-Y. Huang, W.-Y. Sean, Reverse osmosis integrated with renewable energy as sustainable technology: a review, Desalination 581 (2024) 117590.
[15] N.R. Sarker, P. Cherukupally, R. Sodhi, A. Bilton, End-of-the-day rinsing for improved maintainability of intermittently operated small-scale photovoltaic-powered reverse osmosis systems, Desalination 599 (2025) 118439.
[16] Z. Cui, Y. Jiang, R. Field, Fundamentals of pressure-driven membrane separation processes, in: Membrane Technology, Elsevier, 2010, pp. 1–18.
[17] S. Sukumar, M. Marsadek, K. Agileswari, H. Mokhlis, Ramp-rate control smoothing methods to control output power fluctuations from solar photovoltaic (PV) sources—a review, Journal of energy storage 20 (2018) 218–229.
[18] S. Li, A. Voigt, A.I. Schäfer, B.S. Richards, Renewable energy powered membrane technology: energy buffering control system for improved resilience to periodic fluctuations of solar irradiance, Renew. Energy 149 (2020) 877–889.
[19] A. González-Moreno, J. Marcos, I. de la Parra, L. Marroyo, Control method to coordinate inverters and batteries for power ramp-rate control in large PV plants: minimizing energy losses and battery charging stress, Journal of Energy Storage 72 (2023) 108621.
[20] K. Iwabuchi, D. Watari, D. Zhao, I. Taniguchi, F. Catthoor, T. Onoye, Enhancing grid stability in PV systems: a novel ramp rate control method utilizing PV cooling technology, Appl. Energy 378 (2025) 124737.
[21] FilmTec, Reverse Osmosis Membranes Technical Manual, 13, 2022.
[22] M.T. Mito, X. Ma, H. Albuflasa, P.A. Davies, Reverse osmosis (RO) membrane desalination driven by wind and solar photovoltaic (PV) energy: state of the art and challenges for large-scale implementation, Renew. Sust. Energ. Rev. 112 (2019) 669–685.
[23] G. Park, A. Schäfer, B.S. Richards, The effect of intermittent operation on a wind-powered membrane system for brackish water desalination, Water Sci. Technol. 65 (5) (2012) 867–874.
[24] B.S. Richards, D.P. Capão, W.G. Früh, A.I. Schäfer, Renewable energy powered membrane technology: impact of solar irradiance fluctuations on performance of a brackish water reverse osmosis system, Sep. Purif. Technol. 156 (2015) 379–390.
[25] W. Lai, Q. Ma, H. Lu, S. Weng, J. Fan, H. Fang, Effects of wind intermittence and fluctuation on reverse osmosis desalination process and solution strategies, Desalination 395 (2016) 17–27.
[26] P. McCormick, H. Suehrcke, The effect of intermittent solar radiation on the performance of PV systems, Sol. Energy 171 (2018) 667–674.
[27] F. Greco, S.G. Heijman, A. Jarquin-Laguna, Integration of wind energy and desalination systems: a review study, Processes 9 (12) (2021) 2181.
[28] W. Liu, et al., Pressure-driven membrane desalination, Nature Reviews Methods Primers 4 (1) (2024) 10.
[29] A. Jossen, J. Garche, D.U. Sauer, Operation conditions of batteries in PV applications, Sol. Energy 76 (6) (2004) 759–769.
[30] S. Hajiaghasi, A. Salemnia, M. Hamzeh, Hybrid energy storage system for microgrids applications: a review, Journal of Energy Storage 21 (2019) 543–570.
[31] E. Ogunniyi, H. Pienaar, Overview of battery energy storage system advancement for renewable (photovoltaic) energy applications, in: 2017 International Conference on the Domestic Use of Energy (DUE), IEEE, 2017, pp. 233–239.
[32] S. Li, A. Voigt, Y.H. Cai, A.I. Schäfer, B.S. Richards, Renewable energy powered membrane technology: energy buffering control to reduce shut-down events and enhance system resilience under different solar days, Advanced Sustainable Systems 7 (7) (2023) 2300031.
[33] D. Villessot, M. Vergnet, T. Garel, D. Vallon, J. Chesneau, Drinking Water Production by Solar Reverse Osmosis: Returns and Performances from Field Operation, TSM. Techniques Sciences Methodes, Genie Urbain Genie Rural (2019) 27–38.
[34] G.L. Park, A.I. Schäfer, B.S. Richards, Renewable energy-powered membrane technology: supercapacitors for buffering resource fluctuations in a wind-powered membrane system for brackish water desalination, Renew. Energy 50 (2013) 126–135.
[35] S. Shivashankar, S. Mekhilef, H. Mokhlis, M. Karimi, Mitigating methods of power fluctuation of photovoltaic (PV) sources–a review, Renew. Sust. Energ. Rev. 59 (2016) 1170–1184.
[36] Ø.S. Klyve, V. Olkkonen, M.M. Nygård, D. Lingfors, E.S. Marstein, O. Lindberg, Retrofitting wind power plants into hybrid PV–wind power plants: impact of resource related characteristics on techno-economic feasibility, Appl. Energy 379 (2025) 124895.
[37] H.M. Maghrabie, A.G. Olabi, A. Rezk, A. Radwan, A.H. Alami, M.A. Abdelkareem, Energy storage for Water desalination systems based on renewable energy resources, Energies 16 (7) (2023) 3178.
[38] V.G. Gude, Energy storage for desalination processes powered by renewable energy and waste heat sources, Appl. Energy 137 (2015) 877–898.
[39] E.O. Ogunniyi, B.S. Richards, Photovoltaic power load-matching challenge in a Reverse Osmosis water desalination system, 2024 IEEE PES/IAS PowerAfrica, Johannesburg, South Africa, 2024, pp. 1–5, https://doi.org/10.1109/PowerAfrica61624.2024.10759408.
[40] A. Dascalu, A.J. Cruden, S.M. Sharkh, Experimental investigations into a hybrid energy storage system using directly connected Lead-acid and Li-ion batteries, Energies 17 (18) (2024) 4726.
[41] C.H.B. Apribowo, S. Sarjiya, S.P. Hadi, F.D. Wijaya, Optimal planning of battery energy storage systems by considering battery degradation due to ambient temperature: a review, challenges, and new perspective, Batteries 8 (12) (2022) 290.
[42] Tesla, PowerWall. https://www.tesla.com/sites/default/files/pdfs/powerwall/Powerwall%202_AC_Datasheet_en_northamerica.pdf. (Accessed 5 February 2024).
[43] A. Du Pasquier, I. Plitz, S. Menocal, G. Amatucci, A comparative study of Li-ion battery, supercapacitor and nonaqueous asymmetric hybrid devices for automotive applications, J. Power Sources 115 (1) (2003) 171–178.
[44] H. Xu, M. Shen, The control of lithium-ion batteries and supercapacitors in hybrid energy storage systems for electric vehicles: a review, Int. J. Energy Res. 45 (15) (2021) 20524–20544.
[45] J. Zhang, M. Gu, X. Chen, Supercapacitors for renewable energy applications: a review, Micro and Nano Eng. 21 (2023) 100229.
[46] Q. Hassan, S. Algburi, A.Z. Sameen, H.M. Salman, M. Jaszczur, A review of hybrid renewable energy systems: solar and wind-powered solutions: challenges, opportunities, and policy implications, Results Eng. 20 (2023) 101621.
[47] J. Porzio, C.D. Scown, Life-cycle assessment considerations for batteries and battery materials, Adv. Energy Mater. 11 (33) (2021) 2100771.
[48] R. Cipollone, D. Di Battista, G. Contaldi, S. Murgia, M. Mauriello, Development of a sliding vane rotary pump for engine cooling, Energy Procedia 81 (2015) 775–783.
[49] CastlePump. "Positive Displacement vs Centrifugal Pumps." https://www.castlepumps.com/info-hub/positive-displacement-vs-centrifugal-pumps/ (accessed on: 02.05.2024).
[50] Grundfos, SQF 0.6–2 N. https://product-selection.grundfos.com/products/sqflex/sqf-06-2-n-95027325?pumpsystemid=2328476622&tab=variant-curves. (Accessed 5 February 2024).
[51] G.L. Park, A.I. Schäfer, B.S. Richards, Renewable energy powered membrane technology: the effect of wind speed fluctuations on the performance of a wind-powered membrane system for brackish water desalination, J. Membr. Sci. 370 (1–2) (2011) 34–44.
[52] C. Caro-Ruiz, et al., Coordination of optimal sizing of energy storage systems and production buffer stocks in a net zero energy factory, Appl. Energy 238 (2019) 851–862.
[53] C.-S. Karavas, K.G. Arvanitis, G. Kyriakarakos, D.D. Piromalis, G. Papadakis, A novel autonomous PV powered desalination system based on a DC microgrid concept incorporating short-term energy storage, Sol. Energy 159 (2018) 947–961.
[54] M.A. Stenhjem, Experimental Study of Hydraulic Accumulator Discharge, NTNU, 2018.
[55] V. Zhuk, O. Verbovskyi, I. Popadiuk, Experimental regulating parameters of bladder-type hydraulic accumulator, International Journal of Applied Mechanics and Engineering 27 (1) (2022) 232–243.
[56] D. Hubner, H. Ortwig, U. Zimmermann, Investigations on Fluid Dynamics of Hydraulic Accumulators, 2016.
[57] L. Xiaohui, C. Shuping, S. Weijie, H. Xiaofeng, Analysis and design of a water pump with accumulators absorbing pressure pulsation in high-velocity water-jet propulsion system, J. Mar. Sci. Technol. 20 (2015) 551–558.
[58] X.T. Ma, A review of the present status of hydraulic accumulator, Appl. Mech. Mater. 246 (2013) 629–634.
[59] A. Sanna, B. Buchspies, M. Ernst, M. Kaltschmitt, Decentralized brackish water reverse osmosis desalination plant based on PV and pumped storage-technical analysis, Desalination 516 (2021) 115232.
[60] J. Mi, et al., Experimental investigation of a reverse osmosis desalination system directly powered by wave energy, Appl. Energy 343 (2023) 121194.
[61] S. Li, M. Milia, A.I. Schäfer, B.S. Richards, Renewable energy powered membrane technology: energy consumption analysis of ultrafiltration backwash configurations, Sep. Purif. Technol. 287 (2022) 120388.
[62] R. Shaik, N. Beemkumar, H. Adharsha, K. Venkadeshwaran, A. Dhass, Efficiency enhancement in a PV operated solar pump by effective design of VFD and tracking system, Materials Today: Proceedings 33 (2020) 454–462.
[63] R. Selvamathi, V. Subramaniyaswamy, V. Indragandhi, Electric Motor Drives and their Applications with Simulation Practices, Academic Press, 2022.

[64] D.E. Mendonça, P.C.M. de Carvalho, P.P. Praça, J.S. Pinheiro, "photovoltaic powered reverse osmosis Plant for Brackish Water without batteries with self acting pressure valve and MPPT," *journal of energy and power*, Engineering 11 (3) (2017).
[65] H.-P. Ma, et al., Reducing fouling of an industrial multi-stage nanofiltration membrane based on process control: a novel shutdown system, J. Membr. Sci. 644 (2022) 120141.
[66] E. Ogunniyi, B.S. Richards, Renewable energy powered membrane technology: Power control management for enhanced photovoltaic-membrane system performance across multiple solar days, Appl. Energy 371 (2024) 123624, https://doi.org/10.1016/j.apenergy.2024.123624.
[67] A. Ramdani, A. Deratani, S. Taleb, N. Drouiche, H. Lounici, Performance of NF90 and NF270 commercial nanofiltration membranes in the defluoridation of Algerian brackish water, Desalination Water Treat 212 (2021) 286–296.
[68] World Health Organisation (WHO), Guidelines for drinking-water quality: incorporating the first and second addenda, World Health Organization, 2022.
[69] A. Sangwongwanich, Y. Yang, and F. Blaabjerg, "A cost-effective power ramp-rate control strategy for single-phase two-stage grid-connected photovoltaic systems," in *2016 IEEE Energy Conversion Congress and Exposition (ECCE)*, 2016: IEEE, pp. 1–7.